Anticontrol of chaos in low-order continuous time systems using neuron

Wallace K.S. Tang and G.Q. Zhong

Department of Electronic Engineering
City University of Hong Kong
Kowloon, Hong Kong
Email: eekstang,eegzhong@ee.cityu.edu.hk

Abstract

A neuron anticontroller is proposed for chaos generation in third-order linear autonomous continuous time systems. With the nonlinear triggering function $f(x) = \tanh(\alpha x)$ of the neuron, chaotic dynamics are observed. Bifurcation analysis and chaos verification are given using numerical continuation techniques and the Shil'nikov theorem.

1. Introduction

Chaotic dynamics are considered to be essential and useful for various engineering applications such as human brain activities [9], network modeling [5], liquid mixing [8], and secure communication [7] and so on. This provides a strong motivation for the current research on a new task of making a non-chaotic dynamical system chaotic, which is known as "anticontrol of chaos". Anticontrolling of chaos with the use of state-feedback [1], small control perturbations or signals [10, 11] were proposed for discrete time systems. However, it is a technical challenge for anticontrolling non-chaotic continuous time systems.

In this paper, a single neuron is proposed as an anticontroller for the generation of chaos from a non-chaotic third-order linear autonomous continuous time system. The bifurcation analysis of the anticontrolled system is given based on the continuation technique using numerical simulation.

The organization of the paper is as follows: In Sect. 2, the neuron anticontroller is described for a third-order linear autonomous continuous system. The theoretical bifurcation analysis on equilibria and periodic orbits are given in Sects. 3 and 4, respectively. Conclusions are finally drawn in Sect. 5.

2. Neuron Feedback System

Consider a general third-order linear autonomous system expressed in its control form of

$$\begin{cases} \dot{x} = y\,, \\ \dot{y} = z\,, \\ \dot{z} = ax + by + cz\,, \end{cases} \tag{1}$$

where a, b, c are constants and $\dot{x} = \frac{dx}{dt}$.

With the assumption that $a, b, c < 0$, a neuron with triggering function $f(x)$ is introduced into the third equation of the system (1):

$$\begin{cases} \dot{x} = y\,, \\ \dot{y} = z\,, \\ \dot{z} = ax + by + cz + f(x)\,, \end{cases} \tag{2}$$

where $f(x) = \tanh(\alpha x)$ and $\alpha > 0$ is a positive constant. The block diagram of the controlled system is depicted in Fig. 1.

Eq. (2) is odd-symmetric and invariant under the mapping $(x, y, z) \mapsto (-x, -y, -z)$. There are three equilibria in Eq. (2):

$$P^0 = (0,0,0) \quad \text{and} \quad P^{\pm} = (q^{\pm}, 0, 0)\,,$$

where $\tanh(\alpha q^{\pm}) = -aq^{\pm}$ with $a < 0$. It is assumed that $\alpha >> |a|$ and hence $q^{\pm} \approx \mp\frac{1}{a}$.

3. Bifurcations of Equilibria

In order to discuss the bifurcations of equilibria, the information about the eigenvalues λ_i at the equilibrium point P^0 are studied. The values of the parameters used for our study are as follows:

$$c = -1,\ \alpha = 10\,.$$

In Figure 2, the following resonant curves are depicted:

$$\begin{aligned} \sigma_1 &: \lambda_1 + \lambda_2 = 0\,, \\ \sigma_2 &: \lambda_2 - \lambda_3 = 0\,, \\ \sigma_3 &: \lambda_2 + \lambda_3 + 2\lambda_1 = 0\,. \end{aligned} \tag{3}$$

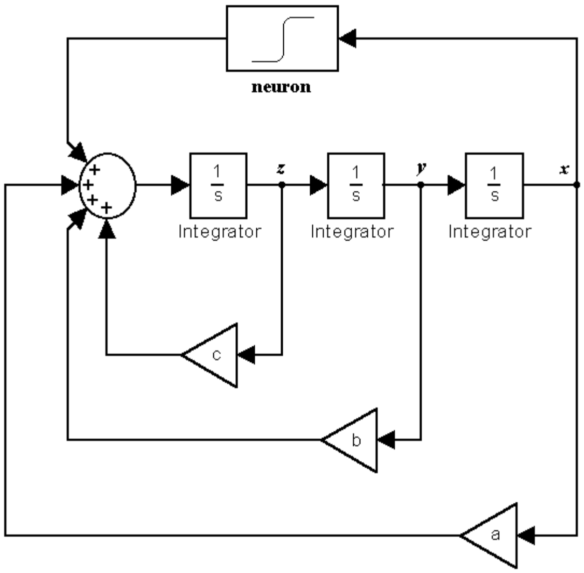

Figure 1: Third-order linear autonomous system with neuron feedback

The Hopf bifurcation curve of $P^{\pm}$ is also plotted and notated as $H^{\pm}$. It is found that the equilibria $P^{\pm}$ undergo an Andronov-Hopf bifurciaton on this curve. The equilibria $P^{\pm}$ are unstable above the curve, with one negative eigenvalue and two eigenvalues with positive real parts. On the other hand, they are stable below the curve $H^{\pm}$. For the equilibrim P^0, it is always unstable but becomes a neurtral saddle on the curve σ_1, having three real eigenvalues with $\lambda_1 = -\lambda_2$.

According to Eq. (3), the equilibrium P^0 is a saddle-focus ($\lambda_1 > 0$, $Re\ \lambda_{2,3} < 0$) if the values of a and b are within the regions below the curve σ_2. The Shil'nikov criteria ($\lambda_1 > |Re\lambda_{2,3}|$) is satisfied if (a, b) is located above the curve $\sigma_3 = 0$. To verify the existence of strange attractor, the principal homoclinic bifurcation curve (as denoted by **Hom** in Fig. 2) is located.

4. One-Parameter Bifurcation for Periodic Orbits

In this section, the bifurcation of the system on the parameter b is studied. It is assumed that

$$a = -1,\ c = -1,\ \alpha = 10\,.$$

A numerical continuation procedure is used to follow the periodic orbits, regardless of their stability. The continuation techniques are based on [3, 4] with the use of AUTO'97 [2].

The bifurcation diagram for periodic orbits in Fig. 3 shows the dependence of the period T on the parameter b. Only the principal symmetric and asymmetric

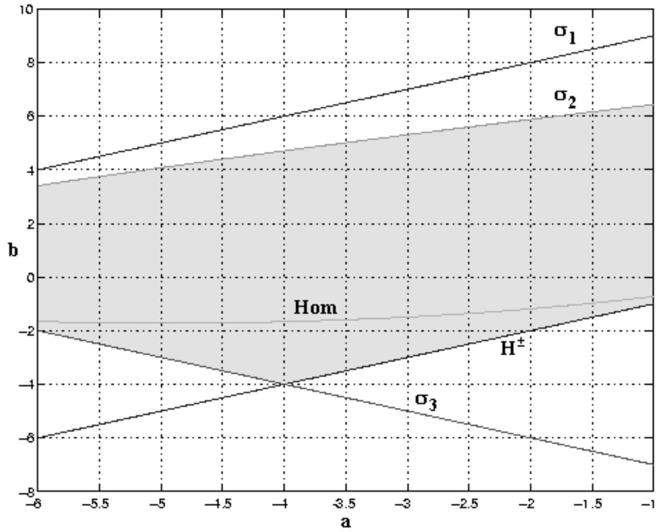

Figure 2: Bifurcation diagram for equilibria, with $c = -1$ and $\alpha = 10$.

periodic orbits, as denoted by "sym" and "asym", respectively, are depicted. For symmetric periodic orbits, half a period ($\frac{T}{2}$) is used.

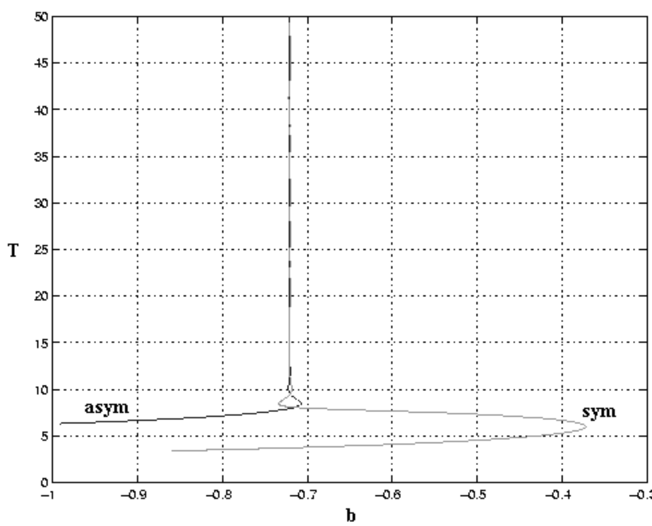

Figure 3: Bifurcation for periodic orbits, with $a = -1$, $c = -1$ and $\alpha = 10$

The branch exhibits a growth of period in a wiggling manner, indicating an unstable saddle-focus loop. The direct consequence of the wiggles on the path of periodic orbits is that several symmetric periodic orbits can exist simultaneously. Similar observation is noticed for the asymmetric branch.

From Fig. 3, a homoclinic orbit of P^0 occurred at the critical value with $b = -0.720558$. There are two homoclinic orbits which are mapped onto each other under the odd symmetry. By solving the characteristic polynomial, the eigenvalues are

$$\lambda_1 = 1.6978,\ \lambda_{2,3} = -1.3489 \pm 1.8658i\,,$$

which means that P^0 is a saddle-focus of Shil'nikov type $(\lambda_1 > |Re(\lambda_{2,3})|)$.

The phase portraits, with increasing values of b, are depicted in Figs. 4-7 to visualize the details of the bifurcation. Initially, only the equilibria $P^{\pm}$ are stable and the system rested at P^+ (or P^-) with a small b. While b increases, an Andronov-Hopf bifurcation occurs when there are two purely imaginary complex conjugate eigenvalues. In our case, it occurs when $b = -1$ for $P^{\pm}$.

As b increases further, the system generates a cascaded period-doubling bifurcation for asymmetric periodic orbits (period-1 and period-2 limit cycles are shown in Figs. 4 and 5, respectively).

At the end of the period-doubling cascade, two asymmetric chaotic attractors (one of them is shown in Fig. 6) emerge and can be observed. These two asymmetric attractors are moving closer and closer toward each other, and eventually "glued" together, giving rise to a double-scroll attractor, as displayed in Fig. 7.

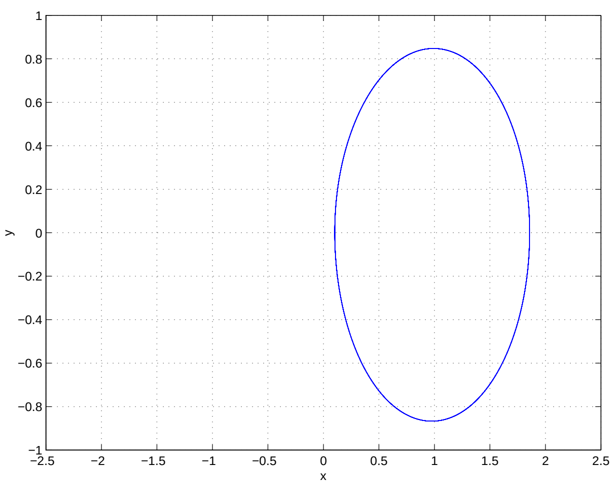

Figure 4: Period-1 limit cycle with $b = -0.95$

The bifurcation diagram for $a = -1$ with increasing b is also depicted in Fig. 8. Besides the above described regimes, some stable symmetric periodic orbits exist as shown in Fig. 9. They persist in some parameter intervals (as shown in Fig. 8). This corresponds to a "periodic window".

5. Conclusion

The ability of introducing a neuron for generating chaos in a third-order linear autonomous continuous

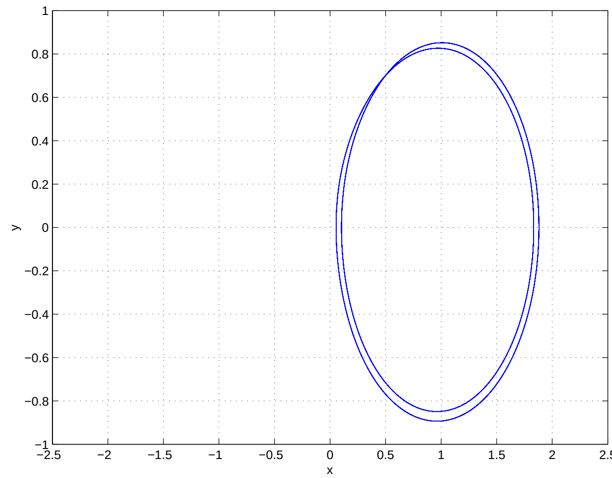

Figure 5: Period-2 limit cycle with $b = -0.92$

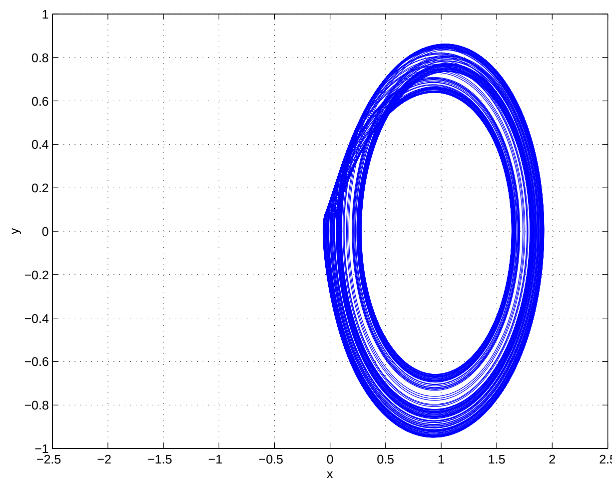

Figure 6: Spiral attractor with $b = -0.864$

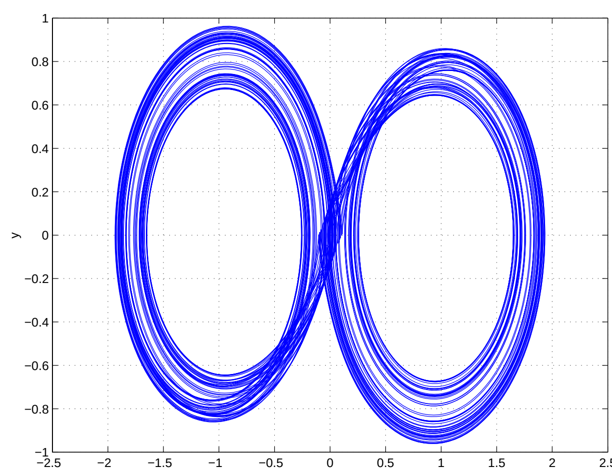

Figure 7: Double scroll attractor with $b = -0.85$

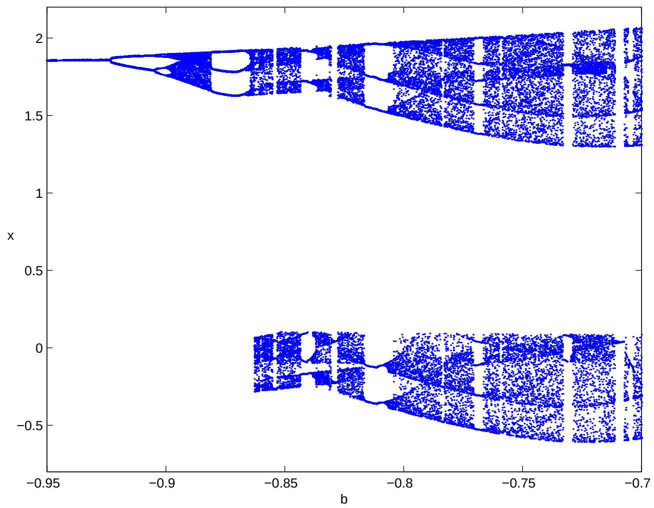

Figure 8: Bifurcation diagram of b, with $a = -1$, $c = -1$ and $\alpha = 10$.

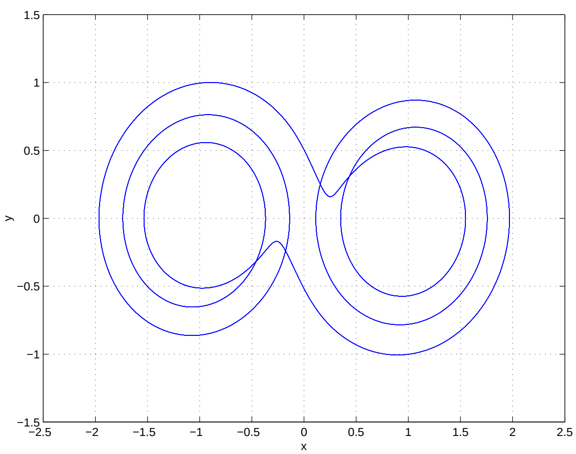

Figure 9: Periodic orbit with $b = -0.81$.

time system is demonstrated. The nonlinear triggering function for the neuron is a hyperbola tangent $f(x) = \tanh(\alpha x)$. The strange attractor has been theoretically verified by means of numerical continuation techniques and the Shil'nikov theorem. Computer simulation has also shown the existence of the strange attractors.

6. Acknowledgements

The work described in this paper was fully supported by the City University of Hong Kong under the Grant No. 7000956.

References

[1] G. Chen and D. Lai, "Feedback anticontrol of discrete chaos," *Int. J. of Bifurcation and Chaos*, vol. 8, 1585-1590, 1998.

[2] E. Doedel, A.R. Champneys, T.F. Fairgrieve, Y.A. Kuznetsov, B. Sandstede, and X. Wang, *AUTO 97: Continuation and Bifurcation Software for Ordinary Differential Equations (with HomCont)*, 1998.

[3] E. Doedel, H.B. Keller and J.P. Kernevez, "Numerical analysis and control of bifurcation problems (I) Bifurcation in finite dimensions," *Int. J. of Bifurcation and Chaos*, vol. 1, no. 3, pp. 493–520, 1991.

[4] E. Doedel, H.B. Keller and J.P. Kernevez, "Numerical analysis and control of bifurcation problems (II) Bifurcation in infinite dimensions," *Int. J. of Bifurcation and Chaos*, vol. 1, no. 4, pp. 745–772, 1991.

[5] A. Erramilli, R.P. Singh and P. Pruthi, "Chaotic maps as models of packet traffic," ITC vol. 14, pp. 329-338, 1994.

[6] A.I. Khibnik, D. Roose and L.O. Chua, "On periodic orbits and homoclinic bifurcaitons in Chua's circuit with a smooth nonlinearity," *Int. J. of Bifurcation and Chaos*, vol. 3, pp. 363–384, 1993.

[7] L. Kocarev, G.M. Maggio, M. Ogorzalek, L. Pecora, K. Yao, (Ed.) "Special Issue: Advances on communication systems using chaos," *IEEE Trans. on Circ. Sys.–I*, vol. 48, no. 12, 2001.

[8] J.M. Ottino, F.J. Muzzio, M. Tjahjadi, J.G. Franjione, S.C. Jana, and H.A. Kusch, "Chaos, symmetry and self-similarity: Exploiting order and disorder in mixing processes," *Science*, vol. 257, pp. 754–760, 1992.

[9] S.J. Schiff, K. jerger, D. H. Duong, T. Chang, M.L. Spano and W.L. Ditto, "Controlling chaos in the brain," *Nature*, vol. 370, pp. 615–620, 1994.

[10] X.F. Wang and G. Chen, "Chaotifying a stable LTI system by tiny feedback control," *IEEE Trans. on Circ. Sys.–I*, vol. 47, no. 3, pp. 410–415, 2000.

[11] W.M.D. Yang, A.J. Mandell and E. Ott, "Preserving chaos: Control strategies to preserve complex dynamics with potential relevance to biological disorders," *Phys. Rev. E*, vol. 51, pp. 102–110, 1995.